

photolysis and trapped as I_2 . (In a typical experiment, irradiation ($\lambda > 600$ nm) of 5.12 mg of $(Cp_2TiI)_2$ (8.4×10^{-6} mol) for 13 h produced 8.8×10^{-6} mol of I_2). When the benzene was removed from the irradiated solution, an air-sensitive green precipitate was left behind that was identical with the green precipitate formed when Cp_2TiI_2

is photolyzed in benzene under purging conditions.

In summary, we propose that Cp_2TiI_2 reacts according to the pathway in Scheme I. The key points are (1) the reactivity involves Ti-I bond cleavage and (2) the loss of the iodine atoms is stepwise with the intermediate formation of $(Cp_2TiI)_2$ in benzene or the formation of $Cp_2Ti(I)Cl$ in CCl_4 . Iodide loss from $(Cp_2TiI)_2$ to give titanocene is possible with a purge of inert gas through the cell to remove I_2 . Otherwise, the I_2 back reacts with the products and no net reaction occurs.

Acknowledgment. This work was generously supported by a University Exploratory Research Grant from the Procter and Gamble Co.

Registry No. Cp_2TiI_2 , 12152-92-0; $Cp_2Ti(I)Cl$, 12116-64-2; $(Cp_2TiI)_2$, 39333-90-9; $[Cp_2Ti(CH_3CN)_2][PF_6]_2$, 94518-22-6; Cp_2TiCl_2 , 1271-19-8; Cp_2Ti , 1271-29-0; I_2 , 7553-56-2; CH_2Cl_2 , 75-09-2; $Ti[PF_6]$, 60969-19-9; acetonitrile, 75-05-8.

$\eta^5-C_5(CH_3)_5$ vs. $\eta^5-C_5H_5$. A Comparison of Electronic Influences for Metallocenes with *fac-a₃b₂c*, *fac-a₃b₃*, and *cis-a₃b₂* Ligand Geometry Based on ^{59}Co NQR Spectroscopy

E. J. Miller, S. J. Landon, and T. B. Brill*

Department of Chemistry, University of Delaware, Newark, Delaware 19716

Received June 18, 1984

^{59}Co NQR data from a series of complexes having *fac-a₃b₂c*, *fac-a₃b₃*, and *cis-a₃b₂* geometry where a_3 is cyclopentadienyl (Cp) or pentamethylcyclopentadienyl ($CpMe_5$) show that $CpMe_5$ inductively donates more electron density than Cp, but the increase felt by the metal is small (<10%). This finding is consonant with conclusions drawn from photoelectron spectroscopy and MO calculations. The electronic effects in $CpCoI_2c$ complexes (c = unidentate donor ligands) having *fac-a₃b₂c* geometry are linear when $CpMe_5$ replaces Cp and are readily explained. The NQR spectra of $CpCo(bb')C_6H_4$ ($b, b' = O, S, N, Se$) complexes having *cis-a₃b₂* geometry are controlled mostly by the electronegativity of b, b' . Replacing Cp by $CpMe_5$ causes a nonlinear variation in the field gradient implying that the electronic structure of complexes with $b = O$ and S differs somewhat from those with $b = N$. The temperature dependence of the coupling constant and asymmetry parameter of $CpMe_5Co(CO)_2$ reveals a phase transition at 177 K but does not indicate a change in the "allyl-ene" distortion of the Cp ring. The field gradient at Co in $CpCob_3$ complexes (b = unidentate donor ligand) is more sensitive to b than to replacement of Cp by $CpMe_5$. This sensitivity is utilized to demonstrate that $P(OCH_3)_3$ is a slightly better electron donor than $P(O)(OCH_3)_2$.

Introduction

Many situations arise in metallocene chemistry where it is advantageous to replace $\eta^5-C_5H_5$ (Cp) with $\eta^5-C_5(CH_3)_5$ ($CpMe_5$).¹ There is no dispute that the replacement of H by CH_3 alters the steric influence of the Cp ring and the solubility of the resultant complex. An increase in electron density along the metal-CpMe₅ bond axis can be expected as a result of inductive donation by CH_3 . The basicity of the $CpMe_5^-$ ring toward H^+ is very much greater than that of Cp^- .² However, photoelectron spectroscopy studies¹ and MO calculations^{3,4} suggest that the electron-releasing nature of the methyl groups is rather small. Moreover, reactions of the $CpMe_5Co^{2+}$ center suggest that the Co(III)

site is still quite hard.⁵ Differences in the reactivity of Cp vs. alkylated Cp complexes may relate more to the transition-state than the ground-state electronic effects.⁶ Another perspective on the redistribution of electron density in metallocenes caused by replacing Cp with $CpMe_5$ as well as by other variations in the molecule evolves from ^{59}Co nuclear quadrupole resonance spectroscopy. Such a study is described here for three ligand geometries and concurs with the previous conclusion that the difference in the inductive electron donation by Cp and $CpMe_5$ is not particularly large.

Cp vs. $CpMe_5$. i. In *fac-a₃b₂c* Complexes. A surprisingly successful model of the electric field gradient (EFG) at cobalt in $CpCoI_2c$ complexes (c = a unidentate ligand) results from viewing the coordination sphere of Co as an octahedron with a geometry of *fac-a₃b₂c*.^{7,8} The Cp

(1) Calabro, D. C.; Hubbard, J. L.; Blevins, C. H.; Campbell, A. C.; Lichtenberger, D. L. *J. Am. Chem. Soc.* 1981, 103, 6839 and references therein.

(2) Bordwell, F. G.; Bausch, M. J. *J. Am. Chem. Soc.* 1983, 105, 6188.

(3) Libit, L.; Hoffmann, R. *J. Am. Chem. Soc.* 1974, 96, 1370.

(4) Schmitz, D.; Fleischhauer, J.; Meier, U.; Schleker, W.; Schmitt, G. *J. Organomet. Chem.* 1981, 205, 381.

(5) Fairhurst, G.; White, C. *J. Chem. Soc., Dalton Trans.* 1979, 1524.

(6) Adams, H.; Bailey, N. A.; White, C. *Inorg. Chem.* 1983, 22, 1155.

(7) Brill, T. B.; Landon, S. J.; Towle, D. K. *Inorg. Chem.* 1982, 21, 1437.

Table I. ^{59}Co NQR Data for Cyclopentadienyl and Pentamethylcyclopentadienyl Complexes of Stoichiometry CpCoI_2c and $[\text{CpCo}_2\text{I}]$ at 298 K

	freq, ^b MHz (CpMe_5)		e^2Qq/h , MHz		η	
	$\nu_3(7/2 \leftrightarrow 5/2)$	$\nu_2(5/2 \leftrightarrow 3/2)$	CpMe_5	Cp^a	CpMe_5	Cp^a
^c						
CO	27.850 (3)	18.498 (2) ^c	131.07 ^c	123.80	0.289 ^c	0.020
	27.850 (3)	18.029 (2) ^c	130.07 ^c		0.090 ^c	
$\text{P}(\text{OC}_6\text{H}_5)_3$	28.608 (17)	19.044 (5)	133.54	129.94 ^c	0.056	0.114 ^c
CNC_6H_5	28.761 (3)	18.939 (3)	134.61	129.34	0.171	0.233
$\text{As}(\text{C}_6\text{H}_5)_3$	31.333 (16)	20.842 (19)	146.29	138.97	0.070	0.078
$\text{NH}_2\text{CH}_2\text{C}_6\text{H}_5$	34.158 (2)	22.748 (2)	159.44	151.52	0.048	0.054
^b ₂						
en ^d	34.086 (2)	22.695 (2)	159.11	151.10	0.053	0.047
phen ^e	34.166 (7)	22.776 (6)	159.44	152.52	0.011	0.012

^a Reference 7. ^b Parenthetical numbers are signal-to-noise ratios. ^c Two crystallographically independent molecules in the asymmetric unit of the cell. ^d en = ethylenediamine. ^e phen = o-phenylenediamine.

ligand is considered to be tridentate and to occupy the a_3 face of the octahedron. The EFG at Co appears, at first sight, to be complicated owing to the low-site symmetry (C_3). However, the problem simplifies because of the orthogonal angles in the coordination sphere and fortuitous counterbalancing of terms in the EFG tensor.⁷ The z principal axis coincides with the Co-c bond provided b and c differ significantly in their contribution to the EFG. If the a_3 and b ligands remain the same in a series of compounds, then the unique ligand c controls the coupling constant, e^2Qq/h , of cobalt. The asymmetry parameter, η , of cobalt is predicted to be very small or zero.⁷

To be sure, the above treatment is an oversimplification because the Cp ligand is not a tripod, and the mixing of the delocalized MO's of Cp with the Cob_2c fragment is complex. However, the success of this model is astonishing in view of NQR data for the $fac\text{-}a_3b_2c$ ligand geometry.⁷ In particular, small values of η at cobalt predicted and found for a series of conventional Lewis bases, c; a predictable correlation exists between e^2Qq/h (^{59}Co) and the σ -donor/ π -acceptor character of c; and e^2Qq/h and η remain essentially constant when b and c are interchanged. This agreement between prediction and experiment instills confidence in using the coordination sphere model to compare the EFG in metallocenes containing CpMe_5 and Cp. The EFG of CpMe_5 complexes of $fac\text{-}a_3b_2c$ geometry (Table I) is higher than that in Cp complexes, and, accordingly, implies that the difference in the electronic effect of Cp and CpMe_5 felt by the cobalt atom is largely independent of the donor/acceptor properties of c. The EFG at cobalt is related to the d orbital populations, N , by eq 1. Previously, it was shown that the bracketed

$e^2Qq/h =$

$$(e^2Qq/h)_0 \left[N_{d_{z^2}} + \frac{N_{d_{xz}} + N_{d_{yz}}}{2} - N_{d_{xy}} - N_{d_{x^2-y^2}} \right] \quad (1)$$

quantity of eq 1 is overall positive in sign in these complexes,⁷ i.e., that the sum of the population of the d_{z^2} , d_{xz} , and d_{yz} orbitals exceeds $d_{x^2-y^2}$ and d_{xy} . The d_{z^2} orbital coincides with the Co-c bond (the z principal axis) for this coordination sphere analysis. In this orientation d_{xz} and either d_{xy} or $d_{x^2-y^2}$ bond to the Cp ring. Since the two appropriate orbitals figure into eq 1 with opposite signs, their contributions partially cancel. Nevertheless, it is clear that the redistribution of electron density in the cobalt d orbitals upon replacing Cp with CpMe_5 results in a net increase in the population of the d_{z^2} , d_{xz} , and d_{yz} orbitals relative to the $d_{x^2-y^2}$ and d_{xy} . Thus the cobalt atom must

have experienced an increase in electron density, but the actual amount is less certain than in the $fac\text{-}a_3b_3$ geometry (vide infra) because the orbital participation in bonding is not simple. The net magnitude of the bracketed quantity in eq 1 appears to increase by 3–7%. Charge density differences of this magnitude agree with MO calculations on these types of molecules⁴ and are in accord with indications from photoelectron spectroscopy that the inductive effect of the methyl groups is relatively small.¹

ii. In $cis\text{-}a_3b_2$ Complexes. The EFG at Co in $cis\text{-}a_3b_2$ or $cis\text{-}a_3bb'$ complexes of the type CpCo_2 was discussed elsewhere in the context of the effect of the b ligands.⁹ The description is extended here to the analogous CpMe_5Co_2 complexes. The properties of the EFG become rather complicated because the z principal axis does not necessarily lie on a bond axis. In its most probable orientation, z is essentially perpendicular to the Cob_2 plane.⁹ Equation 1 can be applied by placing the d_{z^2} orbital and the z axis in coincidence. The d_{xy} orbital largely forms the Co-b σ bond and has an important role in the Co-Cp bond. The d_{xz} orbital becomes part of a strongly bonding MO with Cp.¹⁰ The NQR spectra indicate that the bracketed quantity in eq 1 is overall positive in these molecules.⁹ The EFG at Co is controlled simply by the sum of the electronegativity of the b ligands. While this correlation was noted earlier,⁹ it is even more convincing with the extension in Figure 2 to include new data for $\text{CpCo}[\text{Se}_2\text{C}_2(\text{C}_6\text{H}_5)_2]$. The difference in the atoms bound to b, b' has very little influence on the EFG at cobalt in these five-membered metallacycles.⁹ The conclusion that the electron density on the cobalt atom is directly controlled by the polarity of the Co-b σ -bond seems inescapable.

One learns more about the electronic structure of these complexes by replacing Cp with CpMe_5 . Table II contains the ^{59}Co coupling constants and asymmetry parameters for this comparison. Because the EFG according to the coordination sphere model involves a composite of the contribution from the a and b sites,⁹ the effect of a on b becomes a factor. Were the EFG at Co a straightforward function of a and b, e^2Qq/h for Cp and CpMe_5 should correlate as the $fac\text{-}a_3b_2c$ data did in Figure 1. The relationship actually found is plotted in Figure 3. When b = chalcogen, the EFG for the CpMe_5 complexes is lower than that for the Cp complexes, while it is about the same when one or both of the b donor atoms is nitrogen. Crystal structure determinations of $\text{CpMe}_5\text{Co}[\text{O}_2\text{C}_6\text{H}_4]$,¹¹ $\text{CpMe}_5\text{Co}[(\text{NH})_2\text{C}_6\text{H}_4]$,¹² and $\text{CpMe}_5\text{Co}[(\text{NH})\text{SC}_6\text{H}_4]$ ¹²

(9) Miller, E. J.; Brill, T. B. *Inorg. Chem.* 1983, 22, 2392.

(10) Gross, M. E.; Troglor, W. C.; Ibers, J. A. *J. Am. Chem. Soc.* 1981, 103, 192.

(11) Miller, E. J.; Rheingold, A. L.; Brill, T. B. *J. Organomet. Chem.* 1984, 273, 377.

Table II. ^{59}Co NQR Data for Cp and CpMe₅ Complexes of Stoichiometry CpCo(bb'C₆H₄) at 298 K

b	b'	freq, ^a MHz (CpMe ₅)		e^2Qq/h , MHz		η	
		$\nu_3(7/2 \leftrightarrow 5/2)$	$\nu_2(5/2 \leftrightarrow 3/2)$	CpMe ₅	Cp ^b	CpMe ₅	Cp ^b
O	O	32.990 (5)	21.148 (7)	156.00	171.71	0.358	0.409
O	NH	34.300 (2)	21.803 (2)	163.18	164.71	0.431	0.209
NH	NH	33.848 (2)	21.544 (11)	160.83	159.03 ^d	0.418	0.193
NH	S	32.161 (5)	20.344 (3)	154.05	155.04	0.498	0.411
S	S ^c	30.788 (4)	19.752 (4)	145.52	151.49 ^d	0.532	0.522
S	Se	30.520 (9)	19.708 (8)	143.79		0.306	
Se	Se ^e				149.04		0.501

^a Parenthetical numbers are signal-to-noise ratios. ^b Reference 7. ^c 1,2-Dithio-4-methylbenzene. ^d Average of two closely spaced coupling constants. ^e Se₂C₂(C₆H₅)₂.

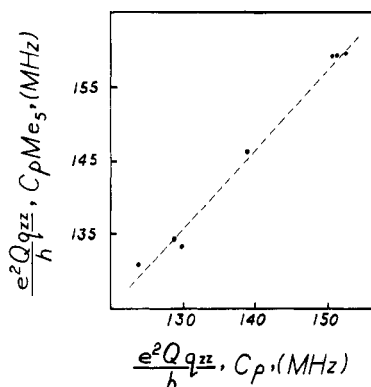


Figure 1. The relationship between the ^{59}Co NQR coupling constants for CpCoI₂c and CpMe₅CoI₂c complexes as a function of the donor ligand c (Table I).

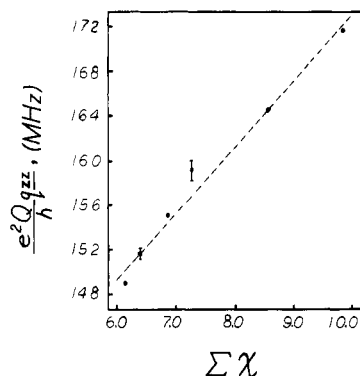


Figure 2. The correlation of the ^{59}Co NQR coupling constant with the sum of the electronegativity of the b, b' atoms in CpCobb' complexes (Table II).

reveal the absence of anomalies in the architecture or bond distances that could explain this difference. It is, therefore, probable that the interplay of subtle electronic differences involving several orbitals is affecting the balance of terms in eq 1. Since the d_{zz} and d_{xy} orbitals of Co predominate in the Cp-Co bond and the bracketed quantity in eq 1 is overall positive in sign, one could anticipate that an equal increase in the electron population of d_{zz} and d_{xy} would diminish e^2Qq/h . This follows because an increase in $N_{d_{xy}}$ reduces the overall magnitude of the bracketed quantity (and thus e^2Qq/h), whereas the other orbital, d_{zz} , enters as $N_{d_{zz}}/2$ and can increase e^2Qq/h by only half as much. The coupling constants for $b_2 = \text{O}$ and S are understandable with this approach.

The situation appears to be slightly different when $b = \text{N}$. The EFG at Co is remarkably insensitive to all substituent variations invoked so far including replacing Cp with CpMe₅ and varying the b, b' ligands through

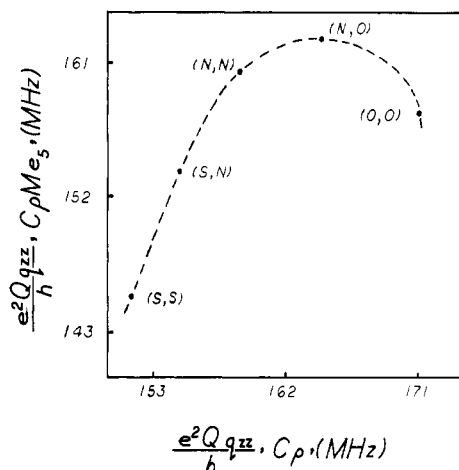


Figure 3. The relationship of the ^{59}Co NQR coupling constants in CpCobb' and CpMe₅Cobb' complexes as a function of b, b'.

(NR)₂C₆H₄ (R = H, CH₃, C₆H₅), and (NC₆H₅)₂N₂.⁹ In all cases, e^2Qq/h lies in the narrow range of 156–161 MHz. Metallacycles formed with diimine ligands have been identified by others^{13–16} as having unusual intramolecular donor-acceptor properties. The NQR data indicate that the electron donor-acceptor behavior of ligands with $b = \text{N}$ attached to CpCo is probably quite flexible and is able to equilibrate electron density in the metal d orbitals so as to leave the bracketed quantity of eq 1 essentially unchanged.

The CpMe₅ behaves as an inductive electron donor in the *cis*-a₃b₂ geometry, but, as in the *fac*-a₃b₂c system, the effect is not large. The electron donation is dampened or compensated for by the other ligands in the coordination sphere. Maitlis¹⁷ has observed that the CpMe₅ ligand is able to donate electron density in proportion to what is needed.

An additional spectroscopic study of CpMe₅ in a *cis*-a₃b₂ complex was stimulated by the suggestion¹⁸ that the C-C bond lengths of CpMe₅Co(CO)₂ at room temperature are consistent with partial localization to the "allyl-ene" electron distribution in the CpMe₅ ring. The NQR spectrum of CpMe₅Co(CO)₂ ($e^2Qq/h = 142.55$ MHz and $\eta = 0.492$ at 295 K) was recorded for comparison with CpCo(CO)₂ ($e^2Qq/h = 157.29$ MHz and $\eta = 0.289$ at 77 K).⁹ While these complexes are formally Co(I) and are not necessarily directly comparable to the *cis*-a₃b₂ complexes

(13) Gross, M. E.; Ibers, J. A.; Trogler, W. C. *Organometallics* 1982, 1, 530.

(14) Gross, M. E.; Trogler, W. C.; Ibers, J. A. *Organometallics* 1982, 1, 732.

(15) Overbosch, P.; van Koten, G.; Spek, A. L.; Roelofsen, G.; Duisenberg, A. J. M. *Inorg. Chem.* 1982, 21, 3908 and references therein.

(16) Overbosch, P.; van Koten, G.; Overbook, O. *J. Am. Chem. Soc.* 1980, 102, 2091.

(17) Maitlis, P. M. *Chem. Soc. Rev.* 1981, 10, 1.

(18) Byers, L. R.; Dahl, L. F. *Inorg. Chem.* 1980, 19, 277.

(12) Miller, E. J.; Rheingold, A. L.; Brill, T. B. *J. Organomet. Chem.*, in press.

Table III. ^{59}Co NQR Data (298 K) for $fac\text{-}a_3b_3$ Complexes Involving $a_3 = \text{Cp}$ or CpMe_5

complex	freq, ^a MHz				e^2Qq/h , MHz		η	
	$\nu_3(7/2 \leftrightarrow 5/2)$		$\nu_2(5/2 \leftrightarrow 3/2)$		Cp	CpMe ₅	Cp	CpMe ₅
	Cp	CpMe ₅	Cp	CpMe ₅				
$\{a_3\text{Co}[\text{P}(\text{OEt})_3]_3\}(\text{BF}_4)$		25.163 (8)		16.763 (13)	117.44		0.039	
$\{a_3\text{Co}[\text{P}(\text{OMe})_3]_3\}(\text{BF}_4)_2$	23.335 (3)	25.113 (3)	15.528 (6)	16.719 (2)	108.94	117.51	0.063	0.055
$\text{K}[a_3\text{Co}(\text{CN})_3]$	27.901 (3)	28.901 (3) ^b	18.178 (6)	19.248 (3) ^b	127.90	134.90	0.090	0.072
$[a_3\text{Co}(\text{CH}_3\text{CN})_3](\text{BF}_4)_2$		33.520 (15)		22.320 (10)	156.47		0.051	

^a Parenthetical numbers are signal-to-noise ratios. ^b Slight differences in the resonance frequencies were observed with different samples and appear in some way to be related to KI impurities. The differences produced in e^2Qq/h are ± 1.0 MHz.

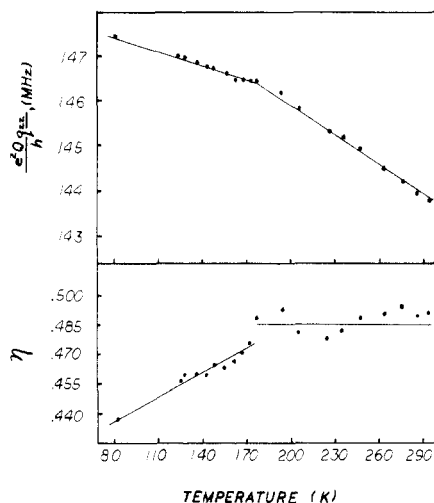


Figure 4. The temperature dependence of the ^{59}Co coupling constant and asymmetry parameter of $\text{CpMe}_5\text{Co}(\text{CO})_2$.

in Table II, the direction of the shift in e^2Qq/h upon replacement of Cp by CpMe_5 is the same. η is substantially larger in $\text{CpMe}_5\text{Co}(\text{CO})_2$. These numbers by themselves are not particularly informative. However, it is possible that the "allyl-ene" structure of the Cp ring could be more pronounced at low temperature as the thermal oscillations diminish. A variable-temperature NQR study was undertaken on $\text{CpMe}_5\text{Co}(\text{CO})_2$. Figure 4 plots e^2Qq/h and η as a function of temperature. The negative temperature coefficient of e^2Qq/h is normal and results from reduction in the torsional oscillations of the molecule as T decreases.¹⁹ A solid-solid phase transition occurs at about 177 K causing slope breaks in e^2Qq/h and η . A more subtle solid-state effect may occur at temperatures around 260 K where the line intensity was observed to diminish. The signals intensify again above and below this temperature. Most importantly, at no temperature do η or e^2Qq/h exhibit a sharp discontinuity that could be attributed to a pronounced change in the structure of the CpMe_5 ring.

iii. In $fac\text{-}a_3b_3$ Complexes. The comparison of Cp and CpMe_5 was expanded to complexes having higher symmetry, namely, the $fac\text{-}a_3b_3$ ligand geometry. In these complexes the z principal axis of the EFG tensor coincides with the C_3 axis which is the vector connecting Co and the centroid (CNT) of the Cp ring. The a and b ligands make equal additive contributions to the EFG.⁸ From the point of view of the d orbitals in eq 1, d_{z^2} coincides with the C_3 axis and d_{xz} and d_{yz} are mostly responsible for Cp-Co and Co-b bonding. The asymmetry parameter must be very small or zero because of the C_3 molecular axis.

The dearth of NQR data for $fac\text{-}a_3b_3$ complexes of cobalt containing Cp and CpMe_5 (Table III) stems from synthetic

difficulties and the inability to find NQR signals in several complexes. We were surprised to discover that replacement of Cp by CpMe_5 produces only a 5–10-MHz increase in e^2Qq/h of Co—about the same magnitude as in the $fac\text{-}a_3b_2c$ ligand geometry. The direction of the shift coincides with that produced at ^{55}Mn by increasing n in $[\text{C}_6\text{H}_{6-n}(\text{CH}_3)_n]\text{Mn}(\text{CO})_3^+$ complexes which also possess $fac\text{-}a_3b_3$ geometry.²⁰ The Mn(I) and Co(III) centers are formally isoelectronic. It was previously established for the Mn(I) series that the sum of the positive terms in eq 1 exceeds the sum of the negative terms.²⁰ The NQR data in Table III suggest the same is true of these Co(III) complexes.

The electron density on Co(III) with a $fac\text{-}a_3b_3$ coordination sphere increases by 5–9% when Cp is replaced by CpMe_5 . On the other hand, the increase is nearly 20% at ^{55}Mn when C_6Me_6 replaces C_6H_6 . This disparity in magnitudes is attributable to the difference in the metal-b bond. The Mn-CO bond is better able to absorb electron density because of the substantial π -acidity of CO, whereas the weaker π -acidity of b in the Co-b bond ($b = \text{CN}^-$, $\text{P}(\text{OR})_3$) makes the metal less of an electron sink. The EFG of Co is very sensitive to b implying that the σ -donor/ π -acceptor differences and charge on b much more strongly influence the orbital population distribution on Co than does replacement of Cp by CpMe_5 . This observation further supports the notion that the electron donor power of CpMe_5 is not large in these molecules, and that permethylated aromatics become better electron donor ligands when the other ligands in the coordination sphere are strong π -acceptors.

$\text{P}(\text{OCH}_3)_3$ vs. $\text{P}(\text{O})(\text{OCH}_3)_2^-$. The sizable perturbation to the EFG caused by b in the $fac\text{-}a_3b_3$ geometry suggests a sidelight study to test not only the interface between the $fac\text{-}a_3b_2c$ and $fac\text{-}a_3b_3$ coordination sphere models of the EFG but also the bonding characteristics of $\text{P}(\text{OMe})_3$ and $\text{P}(\text{O})(\text{OMe})_2^-$ that are of recent interest to us.^{21–24} Note that the direction of the z principal axis of the EFG is very different in these two coordination sphere geometries so that when a $fac\text{-}a_3b_3$ complex is converted to a $fac\text{-}a_3b_2c$ complex by ligand substitution, irregular variations in the EFG might be induced. On the other hand, if the EFG contributions from b and c are very similar, the z axis might remain close to the Co-CNT vector in both geometries.

$\text{CpCo}[\text{P}(\text{OMe})_3]_{3-n}[\text{P}(\text{O})(\text{OMe})_2]_n$, $n = 0\text{--}3$, is a directly comparable series of $fac\text{-}a_3b_3$ and $fac\text{-}a_3b_2c$ complexes. Abrupt differences in the EFG might be anticipated if the orientation of the z principal axis shifts dramatically with n . If the direction of z is invariant, then a smooth trend

(20) Brill, T. B.; Kotlar, A. J. *Inorg. Chem.* 1974, 13, 470.

(21) Towle, D. K.; Landon, S. J.; Brill, T. B.; Tulip, T. H. *Organometallics* 1982, 1, 295.

(22) Landon, S. J.; Brill, T. B. *J. Am. Chem. Soc.* 1982, 104, 6571.

(23) Landon, S. J.; Brill, T. B. *Inorg. Chem.* 1984, 23, 1266.

(24) Landon, S. J.; Brill, T. B. *Inorg. Chem.*, in press.

(19) Kushida, T.; Benedek, G. B.; Bloembergen, N. *Phys. Rev.* 1956, 104, 1364.

Table IV. ^{59}Co NQR Data (298 K) Comparing the *fac-a_3b_3* and *fac-a_3b_2c* Ligand Geometries Produced in the CpCo Fragment When $b, c = \text{P}(\text{OMe})_3$ and $\text{P}(\text{O})(\text{OMe})_2^-$

complex	freq, ^a MHz		e^2Qq/h , MHz	η
	$\nu_3(7/2 \leftrightarrow 5/2)$	$\nu_2(5/2 \leftrightarrow 3/2)$		
CpCo[P(OMe) ₃] ₃ (BF ₄) ₂	23.335 (3)	15.528 (6)	108.94	0.063
CpCo[P(OMe) ₃] ₂ [P(O)(OMe) ₂] ₂	22.482 (11)	14.590 (5)	105.71	0.273
CpCo[P(O)(OMe) ₂] ₃ H	21.620 (2)	14.321 (3)	101.03	0.120

^a Parenthetical numbers are signal-to-noise ratios.

in the EFG should be observed. Table IV presents the data now available ($n = 0, 2, 3$). CpCo[P(O)(OMe)₂]₃H and CpCo[P(OMe)₃]₂²⁺ possess the *fac-a_3b_3* geometry and define the limits of e^2Qq/h for ^{59}Co in this series. The *fac-a_3b_2c* complex CpCo[P(OMe)₃]₂[P(O)(OMe)₂]₂ has an intermediate value of the EFG, suggesting that, despite the difference in geometry, the z axis of the EFG tensor is positioned similarly in all three complexes. This will occur only if the EFG produced by P(OMe)₃ resembles that of P(O)(OMe)₂⁻. The gradual decrease in the EFG as n increases shows that P(O)(OMe)₂⁻ is a slightly poorer σ -donor and/or π -acceptor toward the cobalt atom than P(OMe)₃. The weaker bond is manifested in a longer metal-P bond for P(O)(OMe)₂⁻ compared to P(OMe)₃ when the same metal center is involved.^{21,25,26}

Experimental Section

Ligands and Reagents. All solvents were reagent grade or better and, except where noted, were used as received. P(OC₆H₅)₃, P(OCH₃)₃, and P(OC₂H₅)₃, (RIC/ROC), NH₂CH₂C₆H₅, *o*-(NH₂)₂C₆H₄, NH₂CH₂CH₂NH₂, *o*-aminothiophenol, 3,4-dithiobenzotoluene, AgBF₄, and As(C₆H₅)₃ (Aldrich) and I₂ and KCN (Fisher) were used without purification. Phenyl isocyanide²⁷ and selenothioacetate²⁸ were prepared as before. *o*-Phenylenediamine (Eastman) was purified by standard procedures,²⁹ while *o*-aminophenol (Aldrich) was sublimed prior to use.

Metal Complexes. $[\eta^5\text{-C}_5(\text{CH}_3)_2\text{Co}(\text{CO})_2]$ was prepared³⁰ from C₅(CH₃)₅H,³¹ Co₂(CO)₈ (Pressure Chemical),³² and 1,3-cyclohexadiene (Aldrich). $[\eta^5\text{-C}_5\text{H}_5\text{CoI}_2(\text{CO})]$ was prepared as before³³ using $(\eta^5\text{-C}_5\text{H}_5)\text{Co}(\text{CO})_2$ (Pressure Chemical). $[\{\eta^5\text{-C}_5(\text{CH}_3)_5\text{Co}(\mu\text{-I})\}_2]$,³⁰ $[\eta^5\text{-C}_5(\text{CH}_3)_5\text{CoI}_2[\text{P}(\text{OC}_6\text{H}_5)_3]]$,⁵ $[\{\eta^5\text{-C}_5(\text{CH}_3)_5\text{Co}[\text{P}(\text{OCH}_3)_3]_3(\text{BF}_4)_2\}]$,⁵ $[\{\eta^5\text{-C}_5(\text{CH}_3)_5\text{Co}[\text{P}(\text{OC}_2\text{H}_5)_3]_3(\text{BF}_4)_2\}]$,⁵ $[\eta^5\text{-C}_5\text{H}_5\text{CoI}_2(\text{CNC}_6\text{H}_5)]$,³⁴ $[\eta^5\text{-C}_5\text{H}_5\text{Co}(\text{CN})_3]$,³⁵ $[\eta^5\text{-C}_5\text{H}_5\text{Co}[\text{P}(\text{OCH}_3)_3]_3(\text{BF}_4)_2]$,³⁶ $[\eta^5\text{-C}_5\text{H}_5\text{Co}[\text{P}(\text{OCH}_3)_3][\text{P}(\text{O})(\text{OCH}_3)_2]]$,²¹ $[\{\eta^5\text{-C}_5\text{H}_5\text{Co}[\text{P}(\text{O})(\text{OCH}_3)_2]_3\text{H}\}]$,³⁷ $[\eta^5\text{-C}_5(\text{CH}_3)_5\text{CoI}_2(\text{CO})]$,³⁰ and $[\eta^5\text{-C}_5(\text{CH}_3)_5\text{Co}(\text{O}_2\text{C}_6\text{H}_4)]$ ¹¹ were prepared by known methods.

$[\eta^5\text{-C}_5(\text{CH}_3)_5\text{CoI}_2(\text{CNC}_6\text{H}_5)]$. CNC₆H₅ (0.24 g, 2.33 mmol) in 10 mL of CH₂Cl₂ was added slowly to $[\eta^5\text{-C}_5(\text{CH}_3)_5\text{CoI}_2(\text{CO})]$ (1.00 g, 2.10 mmol) in 30 mL of CH₂Cl₂. The resultant brown solution was stirred for 2 h and reduced to dryness under vacuum at room temperature. The residue was chromatographed on silica gel (2 ft × 3/4 in. column) by using CH₂Cl₂. The first band (pink) was discarded. A second band (brown) upon reducing to dryness under

vacuum at room temperature produced 0.83 g (1.51 mmol, 71.7%) of $[\eta^5\text{-C}_5(\text{CH}_3)_5\text{CoI}_2(\text{CNC}_6\text{H}_5)]$: mp 195–196 °C dec; ¹H NMR (CDCl₃) δ 7.50 (b s, C₆H₅, 5), 2.15 (s, CH₃, 15); ¹³C{¹H} (CDCl₃) δ 156.37, 129.68, 129.35, 128.27, 125.87 (C₆H₅), 96.28 (C₅(CH₃)₅), 11.45 (C₅(CH₃)₅); IR $\nu_{\text{C=O}}$ 2160 cm⁻¹. Anal. Calcd for C₁₇H₂₀CoI₂N: C, 37.05; H, 3.65. Found: C, 36.85; H, 3.80.

$[\{\eta^5\text{-C}_5(\text{CH}_3)_5\text{CoI}(\text{H}_2\text{NC}_2\text{H}_4\text{NH}_2)\}_2]$. This complex was prepared in the same manner as the C₅H₅ analogue³⁸ and yielded black crystals (58% yield), mp 204–207 °C dec. Anal. Calcd for C₁₂H₂₂CoI₂N₂: C, 28.37; H, 4.56. Found: C, 29.15; H, 4.99.

$[\{\eta^5\text{-C}_5(\text{CH}_3)_5\text{CoI}[\text{o}-(\text{NH})_2\text{C}_6\text{H}_4]\}_2]$. This material was prepared in the same manner as the C₅H₅ analogue³⁸ yielding black microcrystals (98% yield): mp 178–180 °C dec; ¹H NMR (CDCl₃) δ 7.25 (m, C₆H₄, 4), 2.23 (s, C₅(CH₃)₅, 15). The amine hydrogen atom was not observed in the ¹H NMR spectrum.

$[\eta^5\text{-C}_5(\text{CH}_3)_5\text{CoI}_2[\text{As}(\text{C}_6\text{H}_5)_3]\cdot\text{CH}_2\text{Cl}_2]$. A CH₂Cl₂ (50 mL) solution of $[\{\eta^5\text{-C}_5(\text{CH}_3)_5\text{Co}(\mu\text{-I})\}_2]$ (0.50 g, 0.56 mmol) and As(C₆H₅)₃ (0.342 g, 1.12 mmol) was stirred for 30 min under N₂ and then evaporated to 25 mL. Hexanes (50 mL) were added, and the resultant solution cooled at 0 °C for 30 min. Upon filtration $[\eta^5\text{-C}_5(\text{CH}_3)_5\text{CoI}_2[\text{As}(\text{C}_6\text{H}_5)_3]\cdot\text{CH}_2\text{Cl}_2]$ (0.53 g, 0.57 mmol, 51% yield) was obtained as dark green crystals: mp 172–175 °C dec; ¹H NMR (CDCl₃) δ 7.20–7.80 (m, C₆H₅, 15), 5.30 (s, CH₂Cl₂, 2), 1.80 (s, C₅(CH₃)₅, 15). Anal. Calcd for C₂₈H₃₀CoI₂As·CH₂Cl₂: C, 41.50; H, 3.84. Found: C, 41.87; H, 3.87. The presence of one CH₂Cl₂ solvate molecule was confirmed by TGA: calcd weight loss 10.1%, found 10.0% at 68 °C.

$[\eta^5\text{-C}_5(\text{CH}_3)_5\text{CoI}_2(\text{NH}_2\text{CH}_2\text{C}_6\text{H}_5)]$. A CH₂Cl₂ (50 mL) solution of $[\eta^5\text{-C}_5(\text{CH}_3)_5\text{CoI}_2(\text{CO})]$ (0.375 g, 0.788 mmol) and H₂NCH₂C₆H₅ (0.169 g, 1.576 mmol) was stirred for 5 h under nitrogen. Evaporation to dryness and recrystallization from a minimum of warm CH₂Cl₂ yielded 0.606 g (1.091 mmol, 69% yield) of green crystals: mp 185–187 °C dec; ¹H NMR (CDCl₃) δ 7.32, 7.26 (s, C₆H₅, 5), 4.17 (b, NH₂, 2), 2.19 (s, CH₂, 2), 1.93 (s, C₅(CH₃)₅, 15). Anal. Calcd for C₁₇H₂₄CoI₂N: C, 36.78; H, 4.36. Found: C, 36.91; H, 4.64.

$[\{\eta^5\text{-C}_5(\text{CH}_3)_5\text{Co}(\text{NCCH}_3)_3(\text{BF}_4)_2\}]$. This complex was prepared by the same method as the PF₆⁻ analogue,⁵ as red crystals (96%): mp 140 °C dec; ¹H NMR (CF₃CO₂H, reference external Me₄Si) δ 2.65 (s, NCCH₃, 9), 1.60 (s, C₅(CH₃)₅, 15); IR $\nu_{\text{C=N}}$ 2332, 2307 cm⁻¹.

$[\{\eta^5\text{-C}_5(\text{CH}_3)_5\text{Co}(\text{CN})_3\}]$. This complex was prepared in the same manner as the C₅H₅³⁸ analogue. The material could not be completely freed of KI impurity but was suitable for NQR analysis. Another synthesis of this complex was reported after this work was completed.³⁹

$[\eta^5\text{-C}_5(\text{CH}_3)_5\text{Co}[\text{S}_2\text{C}_6\text{H}_3\text{CH}_3]]$. A CH₂Cl₂ (50 mL) solution of $[\eta^5\text{-C}_5(\text{CH}_3)_5\text{CoI}_2(\text{CO})]$ (2.00 g, 4.20 mmol) and (HS)₂C₆H₃CH₃ (0.66 g, 4.20 mmol) was vigorously stirred with an aqueous solution (50 mL) of NaC₂H₃O₂ (10 g) for 1.5 h. The aqueous layer was then separated and washed with CH₂Cl₂ (50 mL, 3 times). The combined organic layers were dried over anhydrous Na₂SO₄, filtered, and reduced to dryness under vacuum at room temperature. The crude product was dissolved in a minimum of CH₂Cl₂ and chromatographed on silica gel (column 1 ft × 3/4 in.) using CH₂Cl₂. A blue mobile band was collected and reduced to 40 mL. Hexanes were added (100 mL), and the resultant solution was reduced to 30 mL under vacuum at 35 °C. After the solution was cooled to room temperature, bronze crystals of $[\eta^5\text{-C}_5(\text{CH}_3)_5\text{Co}[\text{S}_2\text{C}_6\text{H}_3\text{CH}_3]]$ (0.93 g, 2.67 mmol, 64%) formed: mp 222 °C; ¹H NMR (CDCl₃) δ 1.90 (s, C₅(CH₃)₅, 15), 2.04 (s, C₆H₃CH₃,

(25) Goh, L.-Y.; D'Aniello, M. J., Jr.; Slater, S.; Muetterties, E. L.; Tavanaiepour, I.; Chang, M. I.; Fredrich, M. F.; Day, V. W. *Inorg. Chem.* **1979**, *18*, 192.

(26) Sullivan, R. S.; Rheingold, A. L.; Landon, S. J.; Brill, T. B., to be submitted for publication.

(27) Weber, W. P.; Gokel, G. W. *Tetrahedron Lett.* **1972**, *17*, 1637.

(28) Pierpont, C. G.; Corden, B.; Eisenberg, R. *J. Chem. Soc. D* **1969**, 401.

(29) Fieser, L. F.; Williamson, K. L. "Organic Synthesis"; D. C. Heath: Boston, MA, 1975; p 325.

(30) Frith, S. A.; Spencer, J. L. *Inorg. Synth.*, in press.

(31) Fagan, P. J.; Schutz, L. D.; Marks, T. J. *Inorg. Synth.* **1982**, *21*, 181.

(32) Purified by dissolving in hexane and filtering under N₂.

(33) Heck, R. F. *Inorg. Chem.* **1965**, *4*, 855.

(34) Powell, E. W.; Mays, M. J. *J. Organomet. Chem.* **1974**, *66*, 137.

(35) Dineen, J. A.; Pausen, R. L. *J. Organomet. Chem.* **1972**, *43*, 209.

(36) Klau, W.; Otto, H.; Eberspach, W.; Buckholz, E. *Chem. Ber.* **1982**, *115*, 1922.

(37) Klau, W.; Dehnicke, K. *Chem. Ber.* **1978**, *111*, 451.

(38) Heck, R. F. *Inorg. Chem.* **1968**, *7*, 1513.

(39) Kollé, U.; Fuss, B. *Chem. Ber.* **1984**, *117*, 753.

3), 7.33 (m, $C_6H_5CH_3$, 3); $^{13}C\{^1H\}$ NMR ($CDCl_3$) δ 10.84 ($C_5(CH_3)_5$), 91.37 ($C_5(CH_3)_5$), 20.85 ($C_6H_5CH_3$), 123.57, 129.48, 129.91, 131.71, 151.99, 155.14 ($C_6H_5CH_3$). Anal. Calcd for $C_{17}H_{21}CoS_2$: C, 58.60; H, 6.08. Found: C, 58.62; H, 6.13.

$[^7^5-C_5(CH_3)_5]Co[(HN)_2C_6H_4]$. A CH_2Cl_2 (50 mL) solution of $[^7^5-C_5(CH_3)_5]CoI_2(CO)$ (0.50 g, 1.05 mmol) and *o*-(NH_2) $_2C_6H_4$ (0.11 g, 1.05 mmol) was vigorously stirred for 5 h with an aqueous solution (50 mL) of NaOH (0.5 g). The aqueous layers was then separated and washed with CH_2Cl_2 (50 mL). The combined organic layers were washed with aqueous NH_4Cl solution (50 mL, 2 times), dried over anhydrous Na_2SO_4 , and filtered. An equal volume of hexanes was added and the solution reduced to dryness under vacuum at room temperature to yield $[^7^5-C_5(CH_3)_5]Co[(HN)_2C_6H_4]$ (0.24 g, 0.81 mmol, 77%). Purification by sublimation at 160 °C (2 mmHg) yielded green crystals: mp 194 °C dec; 1H NMR ($CDCl_3$) δ 2.05 (s, $C_5(CH_3)_5$, 15), 6.83 (s, C_6H_4 , 4), 8.30 (b, NH, 2); $^{13}C\{^1H\}$ NMR ($CDCl_3$) δ 10.33 ($C_5(CH_3)_5$), 85.33 ($C_5(CH_3)_5$), 114.94, 117.60, 149.89 (C_6H_4). Anal. Calcd for $C_{16}H_{21}CoN_2$: C, 63.99; H, 7.05; N, 9.33. Found: C, 64.60; H, 6.99; N, 9.47.

$[^7^5-C_5(CH_3)_5]Co[(HN)(S)C_6H_4]$. A CH_2Cl_2 (150 mL) solution of $[^7^5-C_5(CH_3)_5]Co[As(C_6H_5)_3]_2$ (1.53 g, 2.03 mmol), *o*-(H_2N)-(HS) C_6H_4 (0.26 g, 2.03 mmol), and $N(C_2H_5)_3$ (0.41 g, 4.07 mmol) was stirred for 1 h at room temperature and then reduced to dryness under vacuum at room temperature. The resultant oily solid was dissolved in a minimum of CH_2Cl_2 and chromatographed on silica gel (column 1.5 ft \times $3/4$ in.) using CH_2Cl_2 . The blue mobile band was collected and evaporated to 25 mL. Hexanes (75 mL) were added, and the solution was reduced to dryness under vacuum at room temperature. The solid obtained was dried under vacuum to produce 0.49 g of $[^7^5-C_5(CH_3)_5]Co[(HN)(S)C_6H_4]$ (1.54 mmol, 75%): mp 173–175 °C, 1H NMR ($CDCl_3$) δ 2.00 (s, $C_5(CH_3)_5$, 15), 6.50–7.65 (m, C_6H_4 , 4), 9.48 (b, NH, 1); $^{13}C\{^1H\}$ NMR ($CDCl_3$) δ 10.48 ($C_5(CH_3)_5$), 88.22 ($C_5(CH_3)_5$), 116.83, 117.10, 123.17, 129.55 (C_6H_4). Anal. Calcd for $C_{16}H_{20}NS$: C, 60.56; H, 6.35. Found: C, 60.34; H, 6.35.

$[^7^5-C_5(CH_3)_5]Co[(HN)OC_6H_4]$. Solvents were dried over molecular sieves and purged with N_2 . Manipulations were carried out in Schlenkware. (H_2N)(HO) C_6H_4 (3.53 g, 32.69 mmol, in anhydrous C_2H_5OH) was added dropwise to $NaOC_2H_5$ (1.50 g, 65.25 mmol, in anhydrous C_2H_5OH). $Na_2[(NH)OC_6H_4]$ thus formed (18 mL, titer: 0.1694 mmol/mL of anhydrous C_2H_5OH , 3.049 mmol) was then slowly added to $[^7^5-C_5(CH_3)_5]CoI_2(CO)$ (1.50 g, 3.15 mmol) in CH_2Cl_2 (350 mL). After being stirred for 24 h, the blue solution was filtered and reduced to dryness under vacuum at room temperature. A stream of N_2 was used to remove residual solvent. Filtration of an anhydrous ether solution of the product followed by recrystallization from hexanes yielded dark purple crystals (0.568 g, 1.95 mmol, 61.9%). The material can be further purified by sublimation of 180–200 °C (\sim 3 mmHg). After completion of this work, another preparation of this complex was reported;³⁹ mp 140 °C dec; 1H NMR ($CDCl_3$) δ 2.04 (s, $C_5(CH_3)_5$, 15), 6.5–7.2 (m, C_6H_4 , 4). Minor impurities (<15%), perhaps resulting from alkylation at N, appear in the NMR spectrum but have not interfered with the NQR study.

$(^7^5-C_5H_5)Co[Se_2C_2(C_6H_5)_2]$.⁴⁰ A decalin (50 mL) solution of $(^7^5-C_5H_5)Co(CO)_2$ (5.32 g, 29.55 mmol) and $(C_6H_5)_2C_2$ (5.27 g, 29.55 mmol) was added dropwise to a refluxing slurry of Se (10.50 g, 132.98 mmol) in decalin (100 mL). After 1 h of reflux, the green solution was vacuum distilled and the residue dissolved in minimum of CH_2Cl_2 and chromatographed (2 times) on alumina (column 16 in. \times $3/4$ in.) with hexane–diethyl ether (1/1, v/v). The purple solid from the blue band was precipitated from diethyl ether by adding hexanes (2.73 g, 5.93 mmol, 20%): mp 237 °C;

1H NMR ($CDCl_3$) δ 5.40 (s, C_5H_5 , 5), 7.25 (s, C_6H_5 , 10); $^{13}C\{^1H\}$ δ NMR ($CDCl_3$) δ 77.97 (C_5H_5), 126.80, 127.70, 129.21, 143.81 (C_6H_5), 169.1 (C_2). Anal. Calcd for $C_{19}H_{15}CoSe_2$: C, 49.59; H, 3.29. Found: C, 49.65; H, 3.31.

$[^7^5-C_5(CH_3)_5]Co[SeSC_6H_4]$. A CH_2Cl_2 solution (100 mL) of $[^7^5-C_5(CH_3)_5]CoI_2(CO)$ (3.0 g, 6.304 mmol) and (HS)(HSe) C_6H_4 (1.25 g, 6.61 mmol) were vigorously stirred with $NaC_2H_3O_2$ (10 g in 50 mL of H_2O) for 2 h. The aqueous layer was separated and washed with CH_2Cl_2 (50 mL). The combined organic layers were washed with H_2O (50 mL, 2 times), dried over anhydrous Na_2SO_4 , filtered, and reduced to dryness under vacuum at room temperature. The solid dissolved in a minimum of CH_2Cl_2 was chromatographed on silica gel (column 1.5 ft \times $3/4$ in.) using CH_2Cl_2 . The blue band was collected and reduced to dryness under vacuum at room temperature, producing purple crystals (1.44 g, 3.77 mmol, 59.8%): mp 180 °C dec; 1H NMR ($CDCl_3$) δ 1.96 (s, $C_5(CH_3)_5$, 15), 7.0–7.5, 7.95–8.40 (b, C_6H_4 , 4); $^{13}C\{^1H\}$ NMR ($CDCl_3$) δ 11.10 ($C_5(CH_3)_5$), 90.92 ($C_5(CH_3)_5$), 122.76, 124.49, 130.36, 132.17, 148.05, 157.65 (C_6H_5); mol wt (mass spectrum) calcd 381.971, found 381.972.

Spectra. The ^{59}Co NQR spectra were recorded on a Wilkes NQR-1A superregenerative oscillator spectrometer at room temperature. The frequencies are accurate to ± 0.005 MHz. Variable-temperature NQR studies were obtained by cooling the sample with blow-off from liquid N_2 using a cell described elsewhere.⁴¹ The temperature (± 1 K) was measured by means of a thermocouple and digital thermometer. The sample was allowed to stabilize at each temperature for 10 min prior to measurement of the spectrum. The 1H NMR spectra were recorded on a Perkin-Elmer R-12B or Bruker WM-250 and are referenced to internal $Si(CH_3)_4$ (δ 0.00) unless otherwise noted. IR spectra were recorded on a Perkin-Elmer 180. Thermogravimetric analysis was performed on a Du Pont 950 TGA instrument under an air atmosphere using a 5 °C min^{-1} heating rate from 25 to 200 °C. Melting points were measured in open capillary tubes. Elemental analysis was performed by Microanalysis, Wilmington, DE.

Acknowledgment. We are grateful to Professors J. L. Spencer (University of Bristol), K. P. C. Vollhardt (University of California, Berkeley), and C. G. Pierpont (University of Colorado) for providing the advice on several syntheses and Professor W. C. Troglor (University of California, San Diego) for helpful discussions.

Registry No. $CpMe_5CoI_2(Co)$, 35886-64-7; $CpMe_5CoI_2(P-(O_6H_5)_3]$, 72339-53-8; $CpMe_5CoI_2(CNC_6H_5)$, 94161-59-8; $CpMe_5CoI_2[As(C_6H_5)_3]$, 94161-60-1; $CpMe_5CoI_2(NH_2CH_2C_6H_5)$, 94161-61-2; $[CpMe_5CoIen]I$, 94161-62-3; $[CpMe_5CoI phen]I$, 94161-63-4; $CpCoI_2(Co)$, 12012-77-0; $CpCoI_2[P(OC_6H_5)_3]$, 80642-49-5; $CpCoI_2(CNC_6H_5)$, 94202-31-0; $CpCoI_2[As(C_6H_5)_3]$, 80642-51-9; $CpCoI_2(NH_2CH_2C_6H_5)$, 33198-58-2; $[CpCoIen]I$, 33291-98-4; $[CpCoIphen]I$, 33195-41-4; $CpMe_5(O_2C_6H_4)$, 93057-69-3; $CpMe_5[(NH)OC_6H_4]$, 90540-96-8; $CpMe_5[(NH)_2C_6H_4]$, 94161-64-5; $CpMe_5[(NH)SC_6H_4]$, 94161-65-6; $CpMe_5(S_2C_6H_3CH_3)$, 94161-66-7; $CpMe_5(SeSC_6H_4)$, 94161-67-8; $CpCo[Se_2C_2(C_6H_5)_2]$, 94161-68-9; $\{CpCo[P(OMe)_3]_3(BF_4)_2\}$, 80737-24-2; $K\{CpCo(CN)_3\}$, 38600-67-8; $\{CpMe_5[P(OEt)_3]_3(BF_4)_2\}$, 72339-65-2; $\{CpMe_5[P(OMe)_3]_3(BF_4)_2\}$, 72339-62-9; $K\{CpMe_5Co(CN)_3\}$, 90541-20-1; $[CpMe_5Co-(CH_3CN)_3](BF_4)_2$, 94161-69-0; $CpCo[P(OMe)_3][P(O)(OMe)_2]$, 79018-66-9; $CpCo[P(O)(OMe)_2]_3H$, 64012-52-8; $\{CpMe_5Co(\mu-I)_2\}$, 72339-52-7; $CpCo(CO)_2$, 12078-25-0; $(C_6H_5)_2C_2$, 501-65-5; Se, 7782-49-2; (H_2N)(HO) C_6H_4 , 95-55-6; $Na_2[(NH)OC_6H_4]$, 30798-41-5; $CpCo(O_2C_6H_4)$, 33195-38-9; $CpCo[(NH)OC_6H_4]$, 33195-97-0; $CpCo[(NH)_2C_6H_4]$, 12133-01-6; $CpCo[(NH)SC_6H_4]$, 33154-55-1; $CpCo(S_2C_6H_3CH_3)$, 33198-57-1.

(40) Vollhardt, K. P. C.; Walborsky, E. C. *J. Am. Chem. Soc.* **1983**, *105*, 5507.

(41) Miller, E. J. Ph.D. Dissertation, University of Delaware, 1984.